Fischer-Tropsch Synthesis in Near-Critical *n*-Hexane: Pressure-Tuning Effects

David J. Bochniak and Bala Subramaniam
Dept. of Chemical and Petroleum Engineering, University of Kansas, Lawrence, KS 66045

For Fe-catalyzed Fischer-Tropsch (FT) synthesis with near-critical n-hexane (P_c = 29.7 bar; T_c = 233.7°C) as the reaction medium, isothermal pressure tuning from 1.2 – 2.4 P_c (for n-hexane) at the reaction temperature (240°C) significantly changes syngas conversion and product selectivity. For fixed feed rates of syngas (H_2/CO = 0.5; 50 std. cm^3/g catalyst) and n-hexane (1 mL/min), syngas conversion attains a steady state at all pressures, increasing roughly threefold in this pressure range. Effective rate constants, estimated assuming a first-order dependence of syngas conversion on hydrogen, reveal that the catalyst effectiveness increases with pressure implying the alleviation of pore-diffusion limitations. Pore accessibilities increase at higher pressures because the extraction of heavier hydrocarbons from the catalyst pores is enhanced by the liquid-like densities, yet better-than-liquid transport properties, of n-hexane. This explanation is consistent with the single α (= 0.78) Anderson-Schulz-Flory product distribution, the constant chain termination probability, and the higher primary product (1-olefin) selectivities (~ 80%) observed at the higher pressures. Our results indicate that the pressure tunability of the density and transport properties of near-critical reaction media offers a powerful tool to optimize catalyst activity and product selectivity during FT reactions on supported catalysts.

Introduction

The Fischer-Tropsch (FT) synthesis reaction is the hydrogenation of carbon monoxide on Fe and Co-based catalysts to produce transportation fuels, as well as chemical intermediates. The FT synthesis involves chain growth characterized by the addition of C_1 units to a hydrocarbon chain, resulting in mainly linear hydrocarbons (olefins, paraffins and oxygenates) spanning a wide carbon number range (C_1-C_{20+}). In recent years, the emphasis in FT synthesis studies has shifted to selectively producing products other than gasoline, such as high purity chemical feedstocks and diesel fuels (Dry, 1996).

Conventional FT synthesis has been performed in both gas- and liquid-phase reaction media. Gas-phase reactions exhibit higher reaction rates and diffusivities when compared to liquid-phase reactions, but are hampered by inadequate heat removal resulting in excessive methane formation (Anderson, 1984). Despite these drawbacks, gas-phase reactors have been used on a commercial scale, mainly due to their ability to produce heavy molecular weight waxes which are then hydrocracked to diesel fuels (Dry, 1981; Adesina, 1996). Liquid-phase reactions have superior heat removal capabilities when compared to gas-phase reactions and are, therefore, able to maintain a constant reaction temperature without deactivation (Kölbel and Ralek, 1980; Bhatt et al., 1995). Additionally, the high molecular weight products are much more soluble in a liquid-phase reaction medium relative to a gas-phase reaction medium. However, liquid-phase FT synthesis suffers from mass-transfer limitations, requiring relatively large reactor volumes. The ideal FT synthesis medium would therefore be one with gas-like transport properties and liquid-like heat capacity and solubility characteristics. Such a desired combination of fluid properties is possible with supercritical (*sc*) reaction media.

Correspondence concerning this article should be addressed to B. Subramaniam.

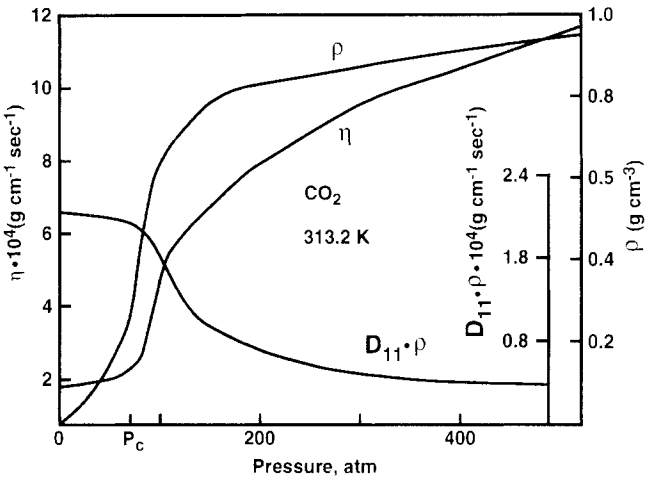

Figure 1. Pressure tunability of solvent and transport properties of near-critical carbon dioxide (Schneider, 1978).

Figure 1 shows the typical variations of density and transport properties of a fluid (CO_2 shown as an example) with pressure along a near-critical isotherm (1.01 T_c). It is clear that the physical and transport properties of the fluid can be altered drastically, from gas-like to liquid-like behavior, simply by isothermally varying the pressure around P_c, the critical pressure. (This pressure-sensitive region is henceforth referred to as the near-critical region.) For example, at pressures slightly above the critical pressure, while the density is roughly 70% of that of the liquid, the diffusivity and viscosity are more gas-like. The solvating power of the reaction mixture is directly related to its density, and, therefore, to its ability to remove hydrocarbons from the catalyst surface. High diffusivities and low viscosities are desirable in reaction media to transport the hydrocarbons out of the catalyst pores before they undergo secondary reactions to form heavier compounds. Thus, by pressure-tuning the fluid properties around the critical pressure, unique combinations of density and transport properties can be realized. An overview of the applications of supercritical reaction media in heterogeneous catalysis may be found elsewhere (Savage et al., 1995; Poliakoff et al., 1997; Dinjus et al., 1997). Supercritical reaction media have been exploited by many groups, including ours, for the *in situ* extraction of coke precursors from catalysts resulting in extended catalyst activity (see Savage et al., 1995 for a review of such applications). In addition, it is also well-known that the heat capacity of fluids passes through a maximum in the near-critical region (Kodra and Balakotaiah, 1992), a property that is especially desirable for absorbing the heat of reaction from highly exothermic reactions such as FT synthesis.

Yokoto and Fujimoto (1989) were the first to report FT investigations with *sc* reaction media. For FT synthesis on a Co catalyst, Yokota and Fujimoto (1989) report superior activity and selectivity in *sc* *n*-hexane (P_c = 29.7 bar; T_c = 233.7°C) compared to either gas (nitrogen) and/or liquid-phase (*n*-hexadecane) reaction media. Subsequent studies have reported that there is an effect on product selectivity when different *sc* reaction media are employed (Yokota et al., 1991; Lang et al., 1995). Bukur and coworkers (Lang et al., 1995; Bukur et al., 1997) report that while syngas conversion on a Fe catalyst was essentially the same whether nitrogen or propane is used as the *sc* reaction medium, the olefin selectivity was considerably higher when propane was used. None of the reported FT studies in *sc* media, however, was aimed at investigating the effects of pressure-tuning the solvent and transport properties of the *sc* reaction medium on FT reaction rates, catalyst activity and product selectivity. Such pressure-tuning studies have merit given that both pore-diffusivities (Iglesia et al., 1991) and the solubilities of the products in the reaction medium (Kuipers et al., 1995) have been cited as influencing the selectivity toward the primary products (viz., the 1-olefins) during FT synthesis in porous catalysts. In the present work, we exploit the pressure-tunable density (viz., solubilizing power) and transport properties (viz., diffusivity and viscosity) of the near-critical reaction medium (*n*-hexane) to examine how isothermal pressure-tuning affects catalyst activity and product selectivity during FT synthesis on a Ruhrchemie iron catalyst. We find that for fixed values of feed composition, weight-hourly space velocity of reactants and reactor temperature, pressure tuning the density and transport properties of near-critical reaction media offers a powerful tool to optimize catalyst activity and product selectivity during FT reactions on supported catalysts.

Experimental Studies

Figure 2 shows the experimental unit. Syngas (32% H_2, 63% CO, and 5% Ar as an internal standard; Matheson Gas Products) was fed through a Brooks 5850E mass-flow controller and then mixed with flowing *n*-hexane fed by a Waters 6000A HPLC pump. The combined stream was then passed through heated lines such that the temperature at the reactor inlet was 240°C. The reactor feed entered at the top of a stainless steel reactor mounted vertically in a sand bath. The reactor is roughly 1.3 cm in ID with a volume of 30 cm^3. The higher temperatures needed during catalyst pretreatment were attained with additional heating elements incorporated into the aluminum blocks that surround the reactor. The inner wall of the reactor was alonized (that is, subjected to an aluminum treatment process) to passivate the stainless steel surface. Due to concerns about the possible catalytic activity of the stainless steel, either glass-lined or silcosteel tubing was installed downstream of the reactor and wherever lines were heated. A computer-actuated stepper-motor controlled micrometering valve maintained the reaction pressure to within ± 0.2 bar of the set point. A profile thermocouple (Omega) with eight equally-spaced thermocouple probes was positioned along the axis of the reactor and used to control the catalyst bed temperature within ± 5°C of the set point. All the measurement and control devices in the reactor unit shown in Figure 2 (viz., thermocouples, pressure transducers, stepping motor controls for driving the micrometering valves, heaters, the mass-flow controller, solid-state relays, solenoid valves) were interfaced with the Camile 2500 data acquisition and control system. Programmed sequences in the data acquisition system facilitated startup and shutdown (normal and emergency) procedures. Additional details of the experimental unit may be found elsewhere (Bochniak, 1997).

An aluminum hot trap equipped with two aluminum, 16 mesh demisters was located immediately downstream of the

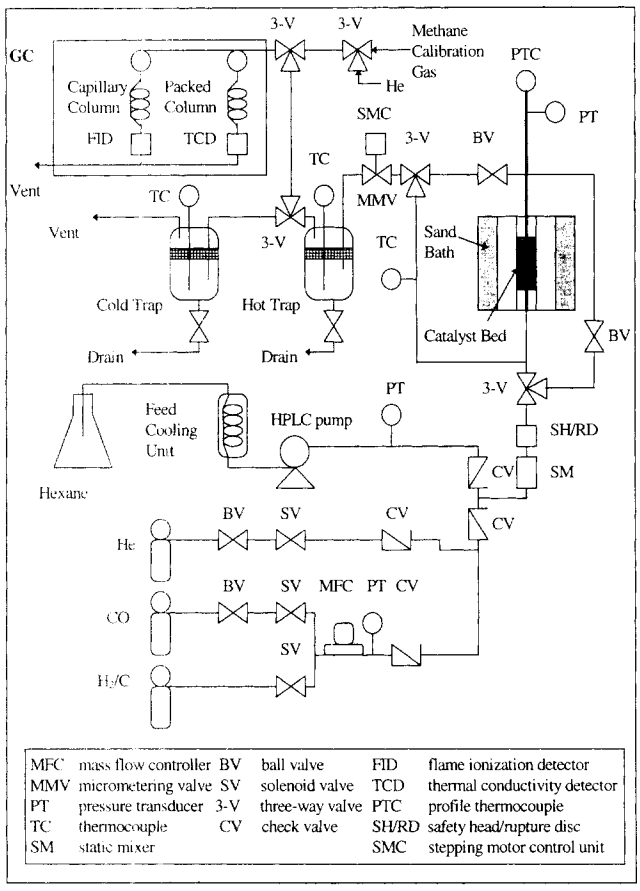

Figure 2. Experimental unit.

micrometering valve. The trap was maintained at 180°C to remove the heavier hydrocarbons (C_{20+}) prior to on-line GC analysis. A HP 5890A gas chromatograph (GC) was used for on-line analysis. The GC was equipped with three columns, two packed columns (HayeSep D), one capillary column (Petrocol DH), a thermal conductivity detector (TCD), and a flame ionization detector (FID). The packed columns enabled quantification of permanent gases and water, while the capillary column measured hydrocarbons (C_1 and higher) and oxygenates (C_1 and above). Details of the analytical system configuration and methodology may be found elsewhere (Snavely and Subramaniam, 1997).

A Ruhrchemie iron catalyst with a composition of 100Fe/5.2Cu/3.7K/10.7Si (mass basis) was used. The cylindrical catalyst pellets were roughly 0.3 cm in diameter and 0.6 cm long. The BET surface area and pore volume of the fresh catalyst (measured with a Micromeretics Gemini 2000 ASAP unit) are 313.1 m^2/g and 0.456 cm^3/g, respectively. The catalyst was pretreated *in situ* as follows: the catalyst bed was first heated to 150°C with helium flowing through the reactor, after which carbon monoxide (Scott Specialty Products, commercial grade) was introduced at 50 sccm. The temperature was then ramped at 1°C/min to 280°C, where it was held for 18 h. Following this hold, the flow was switched back to helium and the reactor was cooled to reaction temperature. The reactor pressure during the pretreatment procedure was 6.9 bar. The BET surface area and pore volume of the pretreated catalyst are 123 m^2/g and 0.143 cm^3/g, respectively. These values are of the same order as those reported in the literature (Dry, 1981).

Experiments were conducted at three different supercritical pressures with respect to *n*-hexane: 35, 55, and 70 bar. All runs were conducted at a temperature of 240°C, a syngas (H_2/CO = 0.5) feed rate of 50 std. cm^3/g catalyst, liquid *n*-hexane flow rate of 1.0 mL/min and a catalyst loading of 1.0 g. The physical and transport properties of *n*-hexane should be tunable from gas-like to liquid-like (that is, by several orders of magnitude) by varying the pressure from 35 to 70 bar at 240°C (1.01 T_c). Each run was continued until the product spectrum had reached a steady state with respect to both syngas conversion and product selectivity. Steady state was deemed to have been attained when product analyses at different times varied less than 5%. Following this, the syngas and *n*-hexane flow were stopped, and the reactor flushed with flowing helium.

Results

Results are discussed in terms of syngas conversion, effective rate constants, carbon number distribution, 1-olefin selectivity, and chain termination probability.

Effects of pressure tuning on syngas conversion and catalyst effectiveness factor

The syngas conversion is estimated as follows using Ar as an internal standard

$$X_s = \frac{(y_{H_2}/y_{Ar} + y_{CO}/y_{Ar})_i - (y_{H_2}/y_{Ar} + y_{CO}/y_{Ar})_O}{(y_{H_2}/y_{Ar} + y_{CO}/y_{Ar})_i} \quad (1)$$

The derivation of Eq. 1 is provided elsewhere (Snavely and Subramaniam, 1997).

Table 1 summarizes the syngas and hydrogen conversions along with the C, H and O balances. The steady-state syngas

Table 1. Conversions, Atomic Balances and Usage Ratio at Steady State*

Pres. (bar)	Conversions (mol %)		Atomic Balances**(%)			Usage Ratio	Wax (C+H) Yield†
	$(CO+H_2)$	H_2	C	H	O	CO/H_2	wt. %
35	15	24	98.2±6.3	85.6±7.6	101.1±6.5	1.14	12.2
55	40	56	93.3±7.5	76.2±5.9	99.0±7.8	0.86	9.3
70	61	67	92.9±9.5	79.3±9.8	98.1±9.9	0.79	5.9

*Catalyst temperature = 240°C; syngas space velocity = 50 std. cm^3/g cat; *n*-hexane flow rate = 1.0 mL/min as liquid; catalyst loading = 1.0 g.
**Based on on-line analysis of effluent stream.
†Based on the total mass of wax collected as a fraction of the total mass of reactants ($CO + H_2$) reacted.

($CO + H_2$) conversion increased with pressure from 18% at 35 bar to 61% at 70 bar. As shown in Table 1, the C and O balances based on on-line analysis of the effluent stream close within experimental error. As reported elsewhere (Snavely and Subramaniam, 1997), only up to C_{15} oxygenates were detected in the on-line analysis suggesting negligible formation, and therefore trapping, of oxygenates in the hot trap held at 180°C. The C balance closure within error suggests that the instantaneous yield and therefore the trapping of C in the heavier (C_{20+}) hydrocarbons should be of the same order as the analysis error. This is indeed confirmed by the "wax" (C_{20+} compounds containing both C and H atoms) yields listed in Table 1, estimated from the overall mass of wax collected in the hot trap during a run. In contrast, the H balance fails to close even after taking analysis error into account. Calculations involving hydrogen balance are more prone to experimental error for the following reasons: (i) the mass of hydrogen reacted during each of the runs summarized in Table 1 is at least an order of magnitude lower than the mass of CO reacted; and (ii) at least two atoms of hydrogen are trapped along with every carbon atom in the hot trap. Based on the C and O balance closures, it should be evident that the on-line analysis of up to C_{20} compounds is reliable.

As shown in Figure 3, the syngas conversion at each pressure reaches a steady state that lasts over the entire duration of the run lasting up to 140 h (not shown in Figure 3) at 55 bar. During these runs, the temperature readings within the catalyst bed remained virtually constant at 240°C as inferred from the profile thermocouple readings. From the steady syngas conversion values, effective rate constants (ηks) were estimated according to the following equation derived assuming a plug-flow reactor and that the syngas conversion is pseudo first-order in H_2 (a valid assumption for syngas conversions less than 60% as shown in Andersen, 1984)

$$\eta k = \left(\frac{F_{So}}{P_T F_{Ao} W}\right)[-F_o \ln(1-X_A) + 2F_{Ao}\{\ln(1-X_A) + X_A\}] \quad (2)$$

Details of the derivation of Eq. 2 may be found in Appendix A. As shown in Figure 4, the effective rate constant increases with pressure from 35 to 55 bar and tends to flatten from 55 to 70 bar wherein the *n*-hexane density also becomes relatively insensitive to pressure. This implies that η (the overall catalyst effectiveness) improves with pressure since the temperature (and hence k, the intrinsic rate constant) is held constant. If the syngas conversion is limited by the external mass-transfer rate, calculations indicate that the external mass-transfer coefficient (and therefore η) should *decrease* at higher pressures. Hence, we interpret the increased effectiveness factor at the higher pressure due to alleviation of pore-diffusion limitations (viz., maintenance of wider pore channels) as a result of enhanced extraction of heavier hydrocarbons from the catalyst pores by the liquid-like densities, yet significantly better-than-liquid diffusivities, of *n*-hexane. Apparently, the positive effects of maintaining wider pore channels enhance *effective* pore-diffusivities, outweighing the decreased bulk diffusivities at the higher pressures.

Fan et al. (1992) studied the effect of catalyst supports with different pore-sizes on supercritical phase Fischer-Tropsch synthesis on supported Ru catalysts. Based on experimental and theoretical studies, Fan et al. reported that when the mean pore size of the support is increased from 84 to 200 Å, the internal catalyst effectiveness factor (η) increases by approximately two- to threefold and the *effective* diffusivities of CO and H_2 increase by roughly five- to sixfold. Thus, based on Fan et al.'s results, the effectiveness factor enhancement observed in the present study (roughly 2.5 times when the pressure is increased from 35 to 70 bar) would correspond to more than a twofold increase in the pore opening (as a result of the enhanced extraction of the heavier hydrocarbons) and a concomitant five- to sixfold increase in the effective diffusivities of CO and H_2.

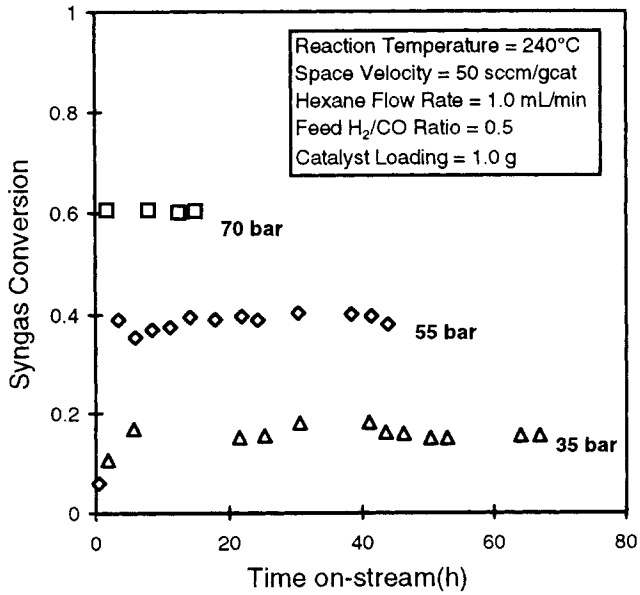

Figure 3. Pressure tuning effects on syngas conversion in near-critical *n*-hexane.

Experimental conditions and conversion values are provided in Table 1.

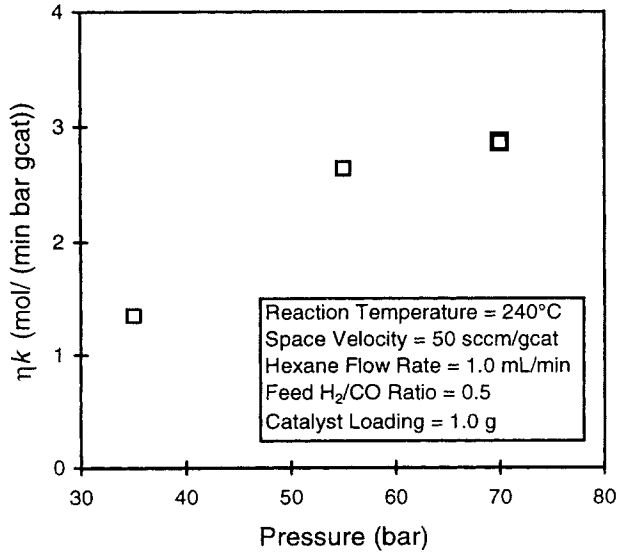

Figure 4. Effect of pressure tuning on catalyst effectiveness factor (η).

The explanation that enhanced extraction of heavier hydrocarbons occurs at the higher pressures is also supported by complementary results on carbon number distribution, 1-olefin selectivity and H_2/CO usage ratio presented in the following sections.

Effects on carbon number distribution

The carbon number distribution of the FT synthesis products is often characterized by a single parameter α, the so-called Anderson-Schulz-Flory (ASF) parameter. A vital assumption behind this characterization is that the probability of adding monomeric C_1 building blocks to an existing carbon chain does not depend upon the carbon number of the product. However, there are several examples of FT studies on Fe, Co, and Ru catalysts where the product distribution does display a dependence upon the carbon number (Iglesia et al., 1991; Madon and Iglesia, 1993) as inferred from the increase in the slope of the ASF plot at higher carbon numbers. Madon and Iglesia (1993) attribute the increased higher molecular weight hydrocarbons to readsorption of 1-olefins onto the catalyst and the subsequent growth of the carbon chain. The readsorption is hypothesized to increase with carbon number due to the decreased diffusivities of larger molecules within a catalyst pore.

In the present study, even though the syngas conversion reached a steady state in eight hours or less, it took significantly longer for a steady product distribution to evolve—from 100 h at 35 bar decreasing to 45 h at 70 bar. Figures 5a–5c show an example of the temporal evolution of the ASF plot at the various pressures. In Figures 5 and 6, normalized mole fraction is defined as the ratio of the moles of all compounds detected within a given carbon number to the total moles of all products detected up to C_{20}. In all cases, the gradual development of a shoulder, starting at C_{10} and extending till C_{15}, was observed. At 35 bar, the shoulder continues to persist (changing less gradually with time) even after 110 h displaying an increasing slope in the C_{10}–C_{19} range (Figure 5a), which is similar to trends observed by research groups at Exxon, MIT, and Texas A&M University as summarized by Donnelly and Satterfield (1989). In contrast, the shoulder gradually disappears with time at 55 bar (Figure 5b) and at 70 bar (Figure 5c). At 55 bar, the shoulder almost (but not quite completely) disappears at the end of the run (44 h, Figure 5b). However, at 70 bar, the shoulder does completely disappear before the end of the run (64.8 h, Figure 5c) resulting in a steady-state carbon number distribution that conforms to the ASF formalism with a *single* α value ($\alpha = 0.78$, Figure 6). This again supports the hypothesis of decreased pore-diffusion limitations at the higher pressures (due to enhanced extraction of the heavier hydrocarbons by the denser

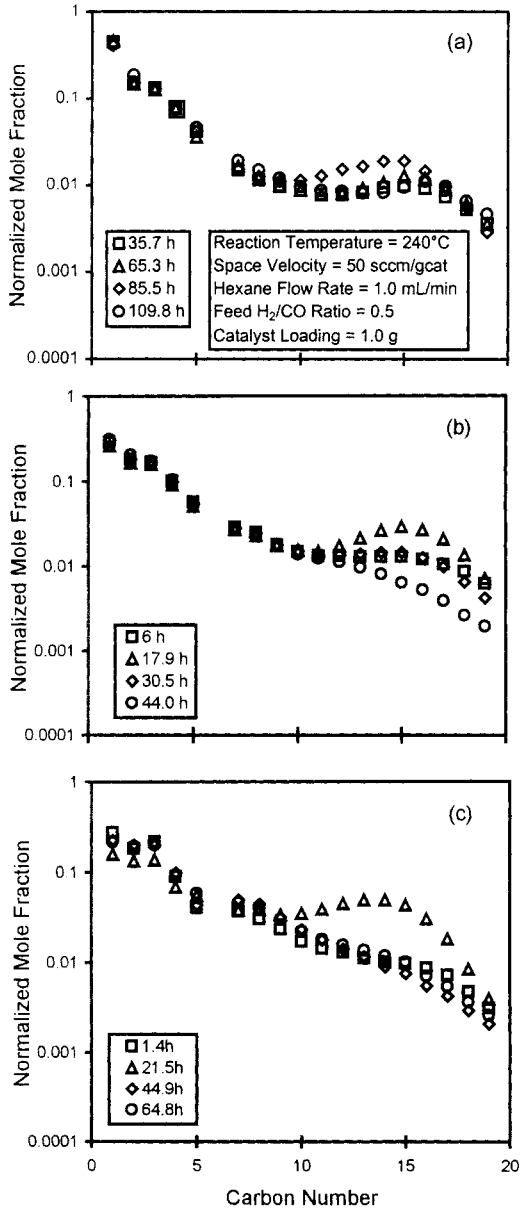

Figure 5. Temporal evolution of the ASF product distribution at the various pressures.

(a) 35 bar; (b) 55 bar; (c) 70 bar.

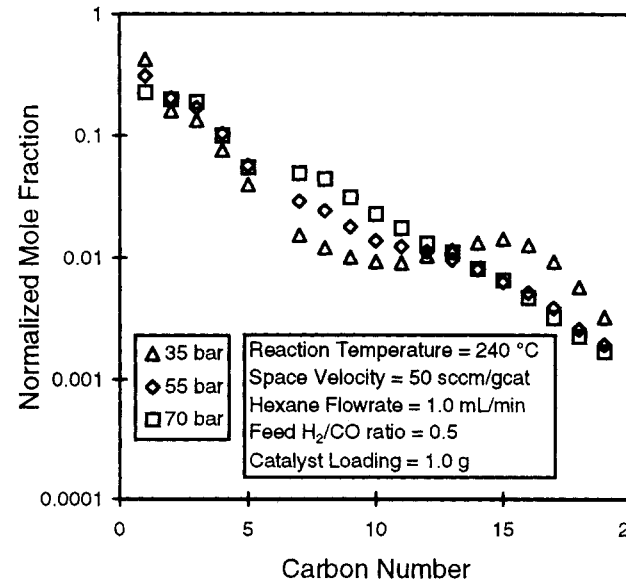

Figure 6. Pressure tuning effects on steady-state ASF product distribution (α).

reaction medium), thus minimizing the readsorption and further reaction of olefins, generally believed to be primary products of the FT synthesis. It also seems plausible that the enhanced solubilities of the heavier hydrocarbons at 55 and 70 bar accelerate the development of a steady ASF product distribution at these pressures relative to 35 bar, wherein the vapor pressures of the C_{10+} hydrocarbons at the reaction temperature and their solubilities in the reaction medium are relatively low, resulting in a slower development of the final steady-state ASF product distribution.

The effect of readsorption on the product distribution may be examined from the chain termination probability for a given carbon number n, β_n, defined as follows (Madon et al., 1991)

$$\beta_n = \frac{\phi_n}{\sum_{i=n+1}^{\infty} \phi_i} \tag{3}$$

where ϕ_n is the mole fraction of species with carbon number n and ϕ_i is the mole fraction of species with carbon number i. If the probability of addition to any given species is the same regardless of carbon number, then β_n should be constant. However, in several studies by the Iglesia-Madon group (Iglesia et al., 1993; Madon and Iglesia, 1993; Madon et al., 1991; Madon et al., 1993), β_n decreased with increasing carbon number, contradicting an important assumption for the ASF carbon number distribution. In sharp contrast, β_n appears more level at higher carbon numbers in our studies at 55 and 70 bar (Figure 7) again reflecting that pore-diffusivities of the reactant and the product molecules and/or their solubilities in n-hexane are significantly influenced by pressure tuning around the critical pressure.

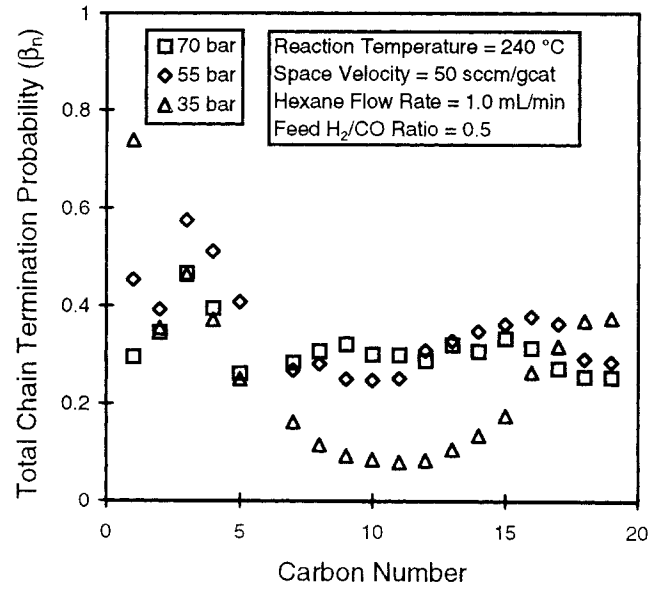

Figure 7. Pressure tuning effects on chain termination probability (β_n)

Effects on 1-olefin selectivity

In recent years, both pore-diffusivities as well as the solubilities of the products in the reaction medium have been cited as influencing the selectivity toward the primary products (viz., the 1-olefins) during FT synthesis in porous catalysts. In general, 1-olefins may undergo secondary reactions such as β-elimination or α-hydrogenation to form the corresponding 2-olefins or paraffins, respectively. In addition, the readsorbed 1-olefins may also undergo chain propagation. Iglesia et al. (1991) and Kuipers et al. (1995) report that the selectivity for 1-olefins decreases with carbon number. Although both studies concur that the extent of secondary reactions is influenced by the likelihood of readsorption of a 1-olefin, they differ in their explanation. Iglesia et al. (1991) relate the degree of olefin readsorption to diffusion limitations within a catalyst pore while Kuipers et al. (1995) opine that the olefin readsorption is influenced by the solubility of the olefins in the reaction medium.

As shown in Figure 8, the 1-olefin selectivity at a given carbon number, ψ (dimensionless) [defined according to Bukur et al. (1997) as the ratio of 1-olefins relative to paraffins, 1- and 2-olefins within a given carbon number] increased with pressure from 35 bar to 55 bar but was virtually unaffected by increasing the pressure from 55 to 70 bar (data overlap), wherein the n-hexane density becomes less sensitive to pressure. The 1-olefin selectivities observed in the present work are greater than those reported with a similar Ruhrchemie catalyst by Bukur et al. (1997), who employed either propane or nitrogen as the reaction medium, either of which has a markedly lower density and hence lower solubilizing power for the olefins when compared to n-hexane. The most striking result, perhaps, is the observation that whereas the 1-olefin selectivities decrease with carbon number at 35 bar in the present study and in the study of Bukur et al. (1997), the steady-state 1-olefin selectivities are virtually constant (within experimental error) with carbon number at 55 and 70

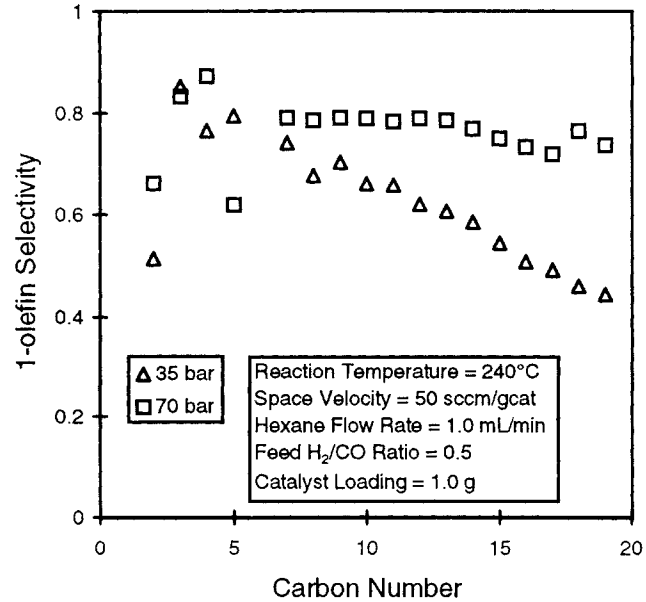

Figure 8. Pressure tuning effects on 1-olefin selectivity (ψ).

bar (roughly 80%). Because the olefin-forming reactions consume less hydrogen relative to either paraffin or oxygenate-forming reactions, the decreased usage ratios (defined as the moles of hydrogen reacted/moles of CO reacted) at the higher pressures (see Table 1) are consistent with the higher olefin selectivities observed at these pressures.

The ability of supercritical reaction media to extract coke precursors (1-olefins occurring as oligomers) *in situ* from porous catalysts (before the oligomers undergo further reaction to consolidated coke) and the concomitant increase in pore accessibilities have been theoretically modeled (Baptist-Nguyen and Subramaniam, 1992) and experimentally observed by several research groups (Tiltscher et al., 1981; Saim and Subramaniam, 1991; Manos and Hofmann, 1991; Dardas et al., 1996). Similar applications are summarized elsewhere (Savage et al., 1995). Thus, the observations of enhanced 1-olefin extraction and the increased pore-diffusivities (that is, catalyst effectiveness) during FT synthesis are consistent with similar observations on other porous catalyst systems.

Conclusions

For Fe-catalyzed Fischer-Tropsch synthesis with near-critical *n*-hexane as the reaction medium, isothermal pressure tuning from 1.2–2.4 P_c in the supercritical region (for *n*-hexane) yields significant changes in syngas conversion and product selectivity. At fixed feed rates of syngas (50 std. cm^3/g catalyst) and *n*-hexane (1 mL/min), syngas composition (H_2/CO = 0.5), catalyst loading (1 g), and catalyst bed-temperature (240°C), syngas conversion attains a steady state at all operating pressures and remains steady throughout the duration of the runs lasting up to 140 h. Syngas conversion increases from 18% at 35 bar to 61% at 70 bar. Evaluation of effective rate constants (based on the pseudo-first-order dependence of syngas conversion on hydrogen) reveals that the catalyst effectiveness increases with pressure implying the alleviation of pore-diffusion limitations at the higher pressures. The increased pore-accessibilities are attributed to the enhanced extraction of the heavier hydrocarbons from the catalyst pores by the liquid-like densities, yet better-than-liquid transport properties, of *n*-hexane at 55 and 70 bar. Consistent with this explanation, we observe at these pressures an ASF product distribution tending to a single α, higher 1-olefin selectivities, and a constant estimated chain termination probability. The enhanced desorption of the primary products (1-olefins) at 55 and 70 bar inhibits secondary reactions such as hydrogenation and/or other chain termination reactions resulting in higher 1-olefin selectivities. The foregoing results are further evidence that operating regimes within the supercritical region, wherein the density and transport properties of the reaction media can be sensitively manipulated/optimized by isothermal pressure-tuning, must be systematically explored in order to maximize the utility of supercritical reaction media for heterogeneous catalytic reactions.

Acknowledgments

The financial support of the Dept. of Energy (grant DE-FG22-92PC92532) and the award of an Amoco Graduate Fellowship to DJB are gratefully acknowledged.

Notation

F_A = molar flow rate of species A (hydrogen), mol/min
F_{Ao} = inlet molar flow rate of A (hydrogen), mol/min
F_o = total inlet molar flow rate, mol/min
F_{So} = inlet molar flow rate of S (syngas), mol/min
F_T = total molar flow rate, mol/min
k = intrinsic rate constant, mol/(min bar g catalyst)
p_A = partial pressure of species A (hydrogen), bar
P_T = total operating pressure, bar
r_S = reaction rate of species S (syngas), mol/(min g catalyst)
T_c = critical temperature, °C
X_A = conversion of species A (hydrogen)
X_S = conversion of species S (syngas)
y_{Ar} = mole fraction of argon
y_{CO} = mole fraction of carbon monoxide
y_{H_2} = mole fraction of hydrogen
W = weight of catalyst, g

Literature Cited

Adesina, A. A., "Hydrocarbon Synthesis via Fischer-Tropsch Reaction: Travails and Triumphs," *Appl. Catal. A: General*, **138**, 345 (1996).

Anderson, R. B., *The Fischer-Tropsch Synthesis*, Academic Press, Orlando, FL (1984).

Baptist-Nguyen, S., and B. Subramaniam, "Coking and Activity of Porous Catalysts in Supercritical Reaction Media," *AIChE J.*, **38**, 1027 (1992).

Bhatt, B. L., R. Frame, A. Hoek, K. Kinnari, V. U. S. Rao, and F. L. Tungate, "Catalyst and Process Scale-up for Fischer-Tropsch Synthesis," *Topics in Catal.*, **2**, 235 (1995).

Bochniak, D. B., "Fischer-Tropsch Synthesis in a Supercritical Fluid Medium," MS Thesis, Univ. of Kansas (1997).

Bukur, D., X. Lang, A. Akgerman, and Z. Feng, "Effect of Process Conditions on Olefin Selectivity during Conventional and Supercritical Fischer-Tropsch Synthesis," *Ind. Eng. Chem. Res.*, **36**, 2580 (1997).

Dardas, Z., M. G. Süer, Y. H. Ma, and W. R. Moser, "A Kinetic Study of *n*-Heptane Catalytic Cracking over a Commercial Y-Type Zeolite Under Subcritical and Supercritical Conditions, *J. Catal.*, **162**, 327 (1996).

Dinjus, E., R. Fornika, and M. Scholz, "Organic Chemistry in Supercritical Fluids," *Chemistry Under Extreme or Non-Classical Conditions*, R. van Eldik and C. D. Hubbard, eds., Wiley, New York, p. 163 (1997).

Donnelly, T., and C. N. Satterfield, "Performance Testing with a Gas-Liquid-Solid System in a Mechanically Stirred Reactor: the Fischer-Tropsch Synthesis," *Appl. Catal.*, **56**, 231 (1989).

Dry, M. E., "The Fischer-Tropsch Synthesis," *Catalysis Science and Technology*, Vol. 1, J. R. Anderson and M. Boudart, eds., Springer-Verlag, Berlin (1981).

Dry, M. E., "Practical and Theoretical Aspects of the Catalytic Fischer-Tropsch Synthesis," *Appl. Catal. A: General*, **138**, 319 (1996).

Fan, L., K. Yokota, and K. Fujimoto, "Supercritical Phase Fischer-Tropsch Synthesis: Catalyst Pore-Size Effect," *AIChE J.*, **38**, 1639 (1992).

Iglesia, E., S. Reyes, and R. Madon, "Transport-Enhanced α-Olefin Readsorption Pathways in Ru-Catalyzed Hydrocarbon Synthesis," *J. Catal.*, **129**, 238 (1991).

Iglesia, E., S. Reyes, R. Madon, and S. Soled, "Selectivity Control and Catalyst Design in the Fischer-Tropsch Synthesis: Sites, Pellets, and Reactors," *Adv. in Catal.*, **39**, 221 (1993).

Kodra, D., and V. Balakotaiah, "Modeling of Supercritical Oxidation of Aqueous Wastes in a Deep-Well Reactor," *AIChE J.*, **38**, 992 (1992).

Kölbel, H. and M. Ralek, "Fischer-Tropsch Synthesis in the Liquid Phase," *Cat. Rev. Sci. Eng.*, **21**, 225 (1980).

Kuipers, E., I. Vinkenburg, and H. Oosterbeek, "Chain-Length Dependence of α-Olefin Readsorption in Fischer-Tropsch Synthesis," *J. Catal.*, **152**, 137 (1995).

Lang, X., A. Akgerman, and D. Bukur, "Steady State Fischer-Tropsch Synthesis in Supercritical Propane," *Ind. Eng. Chem. Res.*, **34**, 72 (1995).

Madon, R., and E. Iglesia, "The Importance of Olefin Readsorption and H_2/CO Reactant Ratio for Hydrocarbon Chain Growth on Ruthenium Catalysts," *J. Catal.*, **139**, 576 (1993).
Madon, R., E. Iglesia, and S. Reyes, "Non-Flory Product Distributions in Fischer-Tropsch Synthesis Catalyzed by Ruthenium, Cobalt and Iron," *Selectivity in Catalysis, Amer. Chem. Soc. Symp. Ser. 517*, S. Suib and M. Davis, eds., p. 383 (1993).
Madon, R., E. Iglesia, and S. Reyes, "Primary and Secondary Reaction Pathways in Ruthenium-Catalyzed Hydrocarbon Synthesis," *J. Phys. Chem.*, **95**, 7795 (1991).
Manos, G., and H. Hofmann, "Coke Removal from a Zeolite Catalyst by Supercritical Fluids," *Chem. Eng. Technol.*, **14**, 73 (1991).
Poliakoff, M., M. W. George, and S. M. Howdle, "Inorganic and Related Chemical Reactions in Supercritical Fluids," *Chemistry Under Extreme or Non-Classical Conditions*, R. van Eldik and C. D. Hubbard, eds., Wiley, New York, p. 189 (1997).
Saim, S., and B. Subramaniam, "Isomerization of 1-Hexene on Pt/γ-Al_2O_3 Catalyst: Reaction Mixture Density and Temperature Effects on Catalyst Activity, Coke Laydown and Catalyst Micromeritics," *J. Catal.*, **131**, 445 (1991).
Savage, P. E., S. Gopalan, T. L. Mizan, C. J. Martino, and E. E. Brock, "Reactions at Supercritical Conditions: Applications and Fundamentals," *AIChE J.*, **41**, 1723 (1995).
Schneider, G. M., "Physicochemical Principles of Extraction with Supercritical Gases," *Angew. Chem. Int. Ed. Engl.*, **17**, 716 (1978).
Snavely, K., and B. Subramaniam, "On-line Gas Chromatographic Analysis of Fischer-Tropsch Synthesis Products Formed in a Supercritical Reaction Medium," *Ind. Eng. Chem. Res.*, **36**, 4413 (1997).
Tiltscher, H., H. Wolf, and J. Schelchshorn, "A Mild and Effective Method for the Reactivation or Maintenance of the Activity of Heterogeneous Catalysts," *Angew. Chem. Int. Ed. Engl.*, **20**, 892 (1981).
Yokota, K., and K. Fujimoto, "Supercritical Phase Fischer-Tropsch Synthesis Reaction," *Fuel*, **68**, 255 (1989).
Yokota, K., Y. Hanakata, and K. Fujimoto, "Supercritical Phase Fischer-Tropsch Synthesis Reaction. 3. Extraction Capability of Supercritical Fluids," *Fuel*, **70**, 989 (1991).

Appendix A

The effective rate constant ($k_e = \eta k$) (mol/(min bar g catalyst) is estimated using the following simplified form of the stoichiometric equation, which implies dominant olefin formation and rapid water-gas shift activity

$$H_2 + 2CO \rightarrow \frac{1}{n}(CH_2)_n + CO_2 \qquad \text{(A1)}$$

Assuming plug-flow behavior and also that the syngas conversion is pseudo first-order in hydrogen (A) partial pressure, the steady-state material balance for syngas may be written as

$$F_{So}\frac{dX_S}{dW} = -r_S = \eta k p_A = k_e p_A \qquad \text{(A2)}$$

Expressing p_A in terms of hydrogen (A) conversion yields

$$p_A = \left(\frac{F_A}{F_T}\right)P_T = \left(\frac{F_{Ao}(1-X_A)}{F_o - 2X_A F_{Ao}}\right)P_T \qquad \text{(A3)}$$

In deriving Eq. A3, it is assumed that the moles of hydrocarbon formed are small relative to the moles of *n*-hexane fed and the other species in the stoichiometry.

Substituting Eq. A3 into Eq. A2 and recognizing that one mole of H_2 reacts for every mole of syngas with composition $H_2/CO = 0.5$ that reacts (that is, $X_S = X_A$), the following expression for ηk is obtained

$$\eta k = \left(\frac{F_{So}}{P_T F_{Ao} W}\right)[-F_o \ln(1-X_A) + 2F_{Ao}\{\ln(1-X_A) + X_A\}] \qquad \text{(A4)}$$

Manuscript received Mar. 4, 1998, and revision received June 8, 1998.